NUMERICAL SIMULATION OF CONVECTIVE HEAT EXCHANGE IN SPHERICAL LAYERS OF AN INCOMPRESSIBLE LIQUID

G. B. Petrazhitskii and N. M. Stankevich

UDC 536.25

Spherical liquid and gas layers are often encountered in systems which require heat removal, and this is the reason for the rather intensive and multi-faceted study of the nature of the heat exchange taking place in them. In particular, there have been a number of experimental studies [1-3] in which the working media considered were water, air, and liquid silicones ($0.7 \leqslant \mathrm{Pr} \leqslant 4148$). These studies have revealed the general characteristics of the heat exchange and the temperature profiles for different ratios of sphere diameters and made possible a classification of flow regimes. An analytic solution of the problem at low Rayleigh numbers is given in [4]. For one group of parameters ($r_2/r_1 = 2$, $\mathrm{Gr} = 10^3$, $\mathrm{Pr} = 0.7$) the distribution of local heat fluxes at the boundaries of the region was given. A description of the method and the results of the numerical investigation of natural convection in spherical gas layers were given in [5]. The investigation was carried out on the basis of a complete system of differential equations written in the variables V', p', ρ', and T' and taking account of compressibility, dissipative processes, and the variation of the physical properties of the gas as functions of temperature. A comparison of the experimental and numerical results indicated good qualitative agreement. However, owing to the complexity of the mathematical model and to certain difficulties caused by the spherical shape, the calculation of one variant of the problem requires a large amount of machine time. Therefore the main attention in [5] was concentrated on determining how the convective process is affected by the dimensionless parameters characteristic of the compressible medium.

In the present study we investigate how the Prandtl number and the geometry of the region influence the development of the flow and the heat transfer in spherical layers filled with a liquid or a gas. To shorten the calculation time, we construct the numerical model on the basis of a system of equations for an incompressible liquid in the Boussinesq approximation.

We consider the flow and the heat transfer in a layer with impenetrable boundaries which is formed by two concentric spheres, whose outer surface ($R' = R_2'$) and inner surface ($R' = R_1'$) are maintained at constant temperatures of T_2' and T_1' respectively.

In vector form the system of equations describing the nonstationary convection has the form

$$\frac{D\mathbf{V}'}{Dt} = -\frac{1}{\rho'}\operatorname{grad}\mathbf{p}' + \nu\nabla^2\mathbf{V}' + g'\beta'(T' - T_1'); \tag{1}$$

$$\rho' c_p' \frac{DT'}{Dt} = \lambda'\nabla^2 T'; \tag{2}$$

$$\operatorname{div}\mathbf{V}' = 0, \tag{3}$$

where $\mathbf{p}'$ is the deviation of the pressure from the statistical pressure $p_1' = p'(T_1')$; $(T' - T_1')$ is the difference between the local temperature and some characteristic temperature; the rest of the symbols are those in common use.

Experimental investigations [1-3] have shown that the convective flow remains axially symmetric and laminar up to Grashof numbers not exceeding 10^7. The axis of symmetry is a vertical axis passing through the center of the concentric spheres. Axial symmetry is also assumed in the construction of the numerical model.

For our further investigations we use a spherical system of coordinates; we assume that its polar axis coincides with the axis of symmetry and that the angular coordinate θ is mea-

Gorkii. Translated from Zhurnal Prikladnoi Mekhaniki i Tekhnicheskoi Fiziki, No. 4, pp. 93-101, July-August, 1984. Original article submitted May 13, 1983.

0021-8944/84/2504-0583$08.50

sured from the downward direction of the vertical ($\theta = -\pi/2$). By virtue of the symmetry, we have $v_\varphi = \partial/\partial\varphi = 0$.

Introducing the stream function by means of the relations

$$v_r = \frac{1}{r^2\cos\theta}\frac{\partial\psi}{\partial\theta}, \quad v_\theta = -\frac{1}{r\cos\theta}\frac{\partial\psi}{\partial r} \tag{4}$$

and performing the transformations customary for two-dimensional problems in hydrodynamics, we write the system of equations (1)-(3) in the following dimensionless form:

$$\frac{\partial\omega}{\partial t} = \frac{2\omega}{r^2\cos^2\theta}\left(\sin\theta\frac{\partial\psi}{\partial r} + \frac{\cos\theta}{r}\frac{\partial\psi}{\partial\theta}\right) - \frac{1}{r^2\cos\theta}\left(\frac{\partial\omega}{\partial r}\frac{\partial\psi}{\partial\theta} - \frac{\partial\psi}{\partial r}\frac{\partial\omega}{\partial\theta}\right) - \tag{5}$$

$$- \mathrm{GrPr}^2 r\cos\theta\left(\cos\theta\frac{\partial T}{\partial r} - \frac{\sin\theta}{r}\frac{\partial T}{\partial\theta}\right) + \mathrm{Pr}\left(\frac{\partial^2\omega}{\partial r^2} + \frac{1}{r^2}\frac{\partial^2\omega}{\partial\theta^2} + \frac{\mathrm{tg}\,\theta}{r^2}\frac{\partial\omega}{\partial\theta}\right);$$

$$\frac{\partial T}{\partial t} = -\frac{1}{r^2\cos\theta}\left(\frac{\partial\psi}{\partial\theta}\frac{\partial T}{\partial r} - \frac{\partial\psi}{\partial r}\frac{\partial T}{\partial\theta}\right) + \frac{\partial^2 T}{\partial r^2} + \frac{1}{r^2}\frac{\partial^2 T}{\partial\theta^2} + \frac{2}{r}\frac{\partial T}{\partial r} - \frac{\mathrm{tg}\,\theta}{r^2}\frac{\partial T}{\partial\theta}; \tag{6}$$

$$\omega = \frac{\partial^2\psi}{\partial r^2} + \frac{1}{r^2}\frac{\partial^2\psi}{\partial\theta^2} + \frac{\mathrm{tg}\,\theta}{r^2}\frac{\partial\psi}{\partial\theta}. \tag{7}$$

Here v_r, v_θ, v_φ are the projections of the velocity vector V' onto the axes r, θ, φ; $\mathrm{Gr} = g'\beta'\Delta T'\delta'^3/\nu'^2$ is the Grashof number; $\mathrm{Pr} = \nu'/a'$ is the Prandtl number; $T = (T' - T_1')/(T_2' - T_1')$ is the temperature.

When we pass to dimensionless variables, we take as the scales of length, velocity, time, and temperature the quanties $\delta' = R_2' - R_1'$, a'/δ', δ'^2/a', $\Delta T' = T_2' - T_1'$, respectively, where a' is the thermal diffusivity.

The solution of the problem is carried out in the region $r_1 \leqslant r \leqslant r_2$, $-\pi/2 \leqslant \theta \leqslant \pi/2$ on the basis of Eqs. (5)-(7) with the boundary conditions

$$\left.\begin{array}{l} T_1 = 0 \text{ for } r = r_1,\ T_2 = 1 \text{ for } r = r_2 \\ \psi = 0, \quad \omega = \partial^2\psi/\partial r^2 \quad \text{for } r = r_1, r_2 \end{array}\right\} - \pi/2 \leqslant \theta \leqslant \pi/2,$$

$$\psi = \omega = \partial T/\partial\theta = 0 \quad \text{for } \theta = \pm\pi/2,\ r_1 < r < r_2.$$

As the initial conditions, we specify the fields of the stream function, the vorticity, and the temperature corresponding to the state of hydrostatic equilibrium of the liquid:

$$t = 0,\ \psi(r, \theta) = \omega(r, \theta) = 0,\ T(r, \theta) = (r - r_1)r_2/r$$

for $r_1 \leqslant r \leqslant r_2$, $-\pi/2 \leqslant \theta \leqslant \pi/2$.

The motion in the layer starts from the equilibrium state with the sudden application of gravitational-field forces. The stationary solution of the system of equations (5)-(7) with the given initial and boundary conditions is obtained by the method of bringing the initial perturbations to a stop as $t \Rightarrow \infty$.

One of the important characteristics of convective heat exchange that is of interest for technical applications is the convection coefficient ε_{conv} which takes account of the fact that there is more heat exchange when there is convection than in the case of pure conduction. In the numerical calculations the convection coefficient is defined as

$$\varepsilon_{conv} = \left(\frac{r_1}{r_2}\right)\langle \mathrm{Nu}_1\rangle = \left(\frac{r_2}{r_1}\right)\langle \mathrm{Nu}_2\rangle,$$

where <Nu> is the average value of the Nusselt number on the inner surface (i = 1) and the outer surface (i = 2), equal to

$$\langle \mathrm{Nu}_i\rangle = \frac{1}{2}\int_{-\pi/2}^{\pi/2}\left(\frac{\partial T}{\partial r}\right)_i \cos\theta d\theta.$$

From Eqs. (5)-(7) with the given initial and boundary conditions it follows that their solution depends on the parameters Gr and Pr and a geometric factor for the region, which in the present problem is taken to be the relative width of the gap, δ/r_1, or the ratio of the radii, $r_2/r_1 = \delta/r_1 - 1$. One result of the numerical solution is the determination of the form of the relation $\varepsilon_{conv} = \varepsilon_{conv}(\mathrm{Ra}, \mathrm{Pr}, \delta/r_1)$, where $\mathrm{Ra} = \mathrm{GrPr}$ is the Rayleigh number.

The system (5)-(7) was solved numerically by the net-point method. The finite-difference scheme was obtained by the balance method, which we had used earlier in calculating the convection of a compressible gas with variable physical properties and described in detail in [5]. The solution of the difference analogs of Eqs. (5) and (6) is found by an explicit scheme using Seidel's method, and the solution of the Poisson equation (7) is found by an implicit scheme of variable directions. The procedure for solving the difference problem may be found in detail in [6].

The formulation of the difference boundary conditions for all the desired functions, except for ω on $r = r_1$, r_2 and for T on the axis of symmetry, is obvious. For the vorticity and the temperature, we established boundary conditions of second-order accuracy [7] on the aforementioned boundaries; at time $t = n\Delta t$ these conditions have the form

$$\omega_{j,i}^{n} = \frac{8\psi_{j,i+1}^{n} - \psi_{j,i+2}^{n}}{2\Delta r^2} \quad \text{for} \quad r = r_1, \ -\pi/2 < \theta < \pi/2,$$

$$T_{j,i}^{n} = (1/3)\left(4T_{j+1,i}^{n} - T_{j+2,i}^{n}\right) \quad \text{for} \quad \theta = \pi/2, \ r_1 < r < r_2,$$

where Δt is the time step, i is the radius number of the node, and j is its angle number.

In the stationary regime, from the previously found fields ψ, we determined from the relations (4) the angular component v_θ and the radial component v_r of the velocity. The derivatives occurring in (4) were approximated by central differences.

The main series of calculations was carried out on a 25 × 25 net with uniform steps in angle and radius; the influence of this net on the accuracy of the solution was estimated by the method of [5].

The time step Δt was chosen on the basis of stability conditions obtained by the Fourier method on the basis of the linearized system of equations (5)-(7) in the range of Grashof numbers, $10^3 \leqslant Gr \leqslant 7 \cdot 10^5$, and the radius ratios, $1.1 \leqslant r_2/r_1 \leqslant 5$, under consideration; for Prandtl numbers in the range $0.71 \leqslant Pr \leqslant 10$, the time step varied between 10^{-2} and 10^{-5}.

The results discussed here relate to the stationary regime and mainly to the case $T_2 > T_1$. The boundary conditions $T_1 > T_2$ were fixed, as a rule, for convenience of comparison of the numerical data with the experimental data, since all the experiments known to the authors had been carried out with a higher temperature on the inner sphere. The ratio r_2/r_1 was varied by changing the radius of the inner sphere while r_2 was kept constant.

Our analysis of the results of the numerical solution showed that for all the Prandtl numbers, radius ratios, and $Gr > 10^5$ under consideration, the principal form of circulation flow is stable single-vortex flow. The motion of the liquid takes place along crescent-shaped trajectories upward along the heated outer surface and downward along the cooled inner surface. For both thick and thin layers, if the Rayleigh numbers are small, there are slow flows with streamlines symmetric with respect to the middle of the region, $r_c = 9.5(r_1 + r_2)$, $\theta = 0$, and the total amount of heat transferred through the layer remains at the level of the pure-conduction regime (the deviation of ε_{conv} from unity does not exceed 5%).

As the Rayleigh number increases, the motion in the layer becomes more intensive. The removal of heat by the flow leads to a longitudinal temperature gradient. The center of the vortex is shifted downward along the angle and moves slightly toward the outer sphere; the larger r_2/r_1 is for Ra = const, the more substantial this shift becomes. Thus, when $r_2/r_1 = 1.1$ ($Ra = 10^4$, Pr = 1.0), the center of the vortex may be regarded with only a small error as coinciding with the central point of the region, while for $r_2/r_1 = 5$ it is at the point $r_i = r_c + 2\Delta r$, $\theta_j = -45°$, where Δr is the step of the net along the radius. Simultaneously with the vortex shift, there is an increase in the dimensions of the stagnation zone, where the Archimedean forces inhibit the motion of the liquid and the heat transfer takes place mainly through conduction. Convection begins to play an increasingly important role in the total heat transfer for all Prandtl numbers under consideration and any geometry, and therefore for sufficiently large values of Ra ($Ra \geqslant 5 \cdot 10^4$) regions with a reverse temperature gradient will be formed. The angular vortices, which, as in [5], appear for $Gr \geqslant 10^4$, Pr = 0.71, $1.4 \leqslant r_2/r_1 \leqslant 3.0$ near the axis of symmetry on the inner sphere ($\theta = +\pi/2$) and the outer sphere ($\theta = -\pi/2$), are not propagated to the entire width of the gap and are small in comparison with the main crescent-shaped vortex. Such flows are usually [1] considered single-vortex flows. Typical pictures of the streamlines and the isotherms of the above-described flows are given in [5]. Analogous flow pictures were observed visually in [1] with all the temperature differences $\Delta T'$ between the spheres that were investigated there for $1.37 \leqslant r_2/r_1 \leqslant 1.72$ ($2 \cdot 10^4 \leqslant Gr \leqslant 3.6 \cdot 10^6$) and with moderate values of $\Delta T'$ for $r_2/r_1 = 2.53; 3.14$.

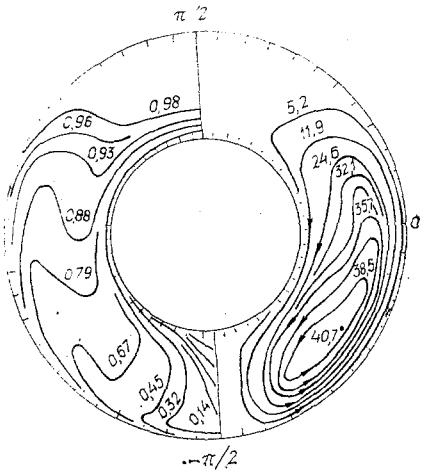

Fig. 1

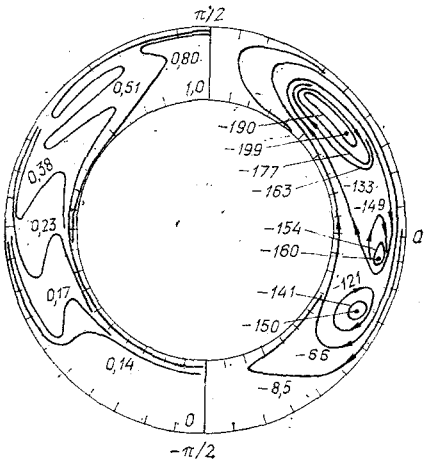

Fig. 2

Comparison with the data of a later experimental study [3] showed that the design structure of the flow for $r_2/r_1 = 1.4$ (Pr = 0.71) in the Grashof-number range $7\cdot10^3 \leqslant Gr \leqslant 1.2\cdot10^4$ does not agree with the flow structure observed in the experiment. The results of the numerical calculations both for $T_2 > T_1$ and for $T_1 > T_2$ indicate that there is a stable crescent-shaped vortex (the angular vortex of [5] for this value of r_2/r_1 appears when $Gr = 2\cdot10^4$), while the experimental data ($T_1 > T_2$) indicate that there is a secondary vortex in the upper part of the region. This vortex has a direction of rotation opposite to that of the main vortex and takes up the entire width of the gap in the radial direction. The authors of [3] assume that when there is a uniform two-dimensional flow, such a vortex cannot be formed constantly and that the flow pictures they obtained are the result of incomplete development of the flow. At the same time, the absence of such a vortex in the numerical experiment, both in a stationary regime and during the entire time required to establish the stationary state, may be due to the fact that a two-dimensional axially symmetric convection model was used.

The influence of the ratio r_2/r_1 on the development of convective flow when $Gr > 10^5$ has been most fully investigated for gases with Pr = 0.71 and 1.0. The picture obtained for the streamlines showed that for large values of r_2/r_1 the flow is not sensitive to the geometry of the region. As the Rayleigh number increases ($10^5 < Ra \leqslant 7\cdot10^5$), the flow remains a single-vortex crescent-shaped flow, which does not contradict the experimental data of [1, 3].

As r_2/r_1 decreases, the influence of the geometry becomes more perceptible. When $r_2/r_1 = 2$, it manifests itself in a transition from a crescent-shaped vortex to a kidney-shaped one. This type of flow is characterized by a distortion of the upper part of the central vortex, which is manifested in a shift of the streamlines of the ascending flow along the radius in the direction of the outer sphere. For Pr = 0.71 the kidney-shaped vortex appears when $Gr = 2.5\cdot10^5$ (Fig. 1). In the experiments of [1, 3] the appearance of this type of flow for air was observed in the range $1.54 \leqslant r_2/r_1 \leqslant 2.17$ when $Gr \approx 2\cdot10^5$.

In narrow gaps ($r_2/r_1 = 1.1$; 1.4), for $Ra > 10^5$ the flow is characterized by a transition from one dominant vortex to a multivortex flow. Stable vortices of low intensity (two at first) are formed starting from $Ra \approx 0.85\cdot10^5$ in the central part of the flow region at the interface between the counterflowing convection currents. As Ra increases, the number of vortices increases, they move further apart, and the flow picture takes on the form seen in Fig. 2 ($T_1 > T_2$, $r_2/r_1 = 1.4$, Pr = 0.71, $Gr = 5\cdot10^5$). The direction of rotation of the secondary vortices coincides with the direction of rotation of the main vortex, which is adjacent to the boundaries of the region. The appearance of such vortices caused by the mutual perturbations of the high-velocity ascending and descending flows was noted in [8] for the case of natural convection of air between two coaxial cylinders. In spherical layers with $r_2/r_1 = 1.4$, Pr = 0.71, and $Gr > 2\cdot10^5$, the authors of [3] observed a nonstationary flow characterized by a three-dimensional spiral vortex in the upper part of the region, the absence of any clearly marked central vortex, and a periodic crowding together of the streamlines in the direction of the outer sphere in the remaining main part of the region. From a comparison of the results of the numerical and the physical experiments it follows that the

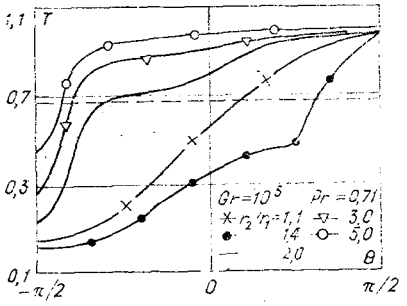

Fig. 3

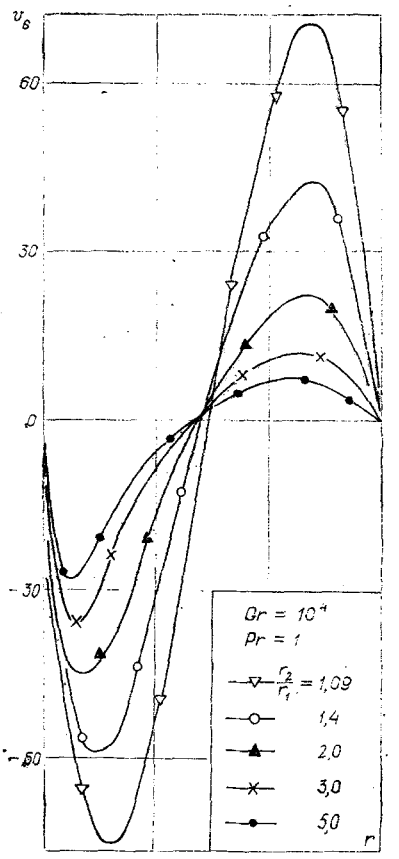

Fig. 4

use of the above-described mathematical model to predict the qualitative picture of the flow in thin layers must evidently be limited by $Gr = 10^4$.

Thus, the numerical calculations have shown that the ratio of radii of the spheres, r_2/r_1, influences both the type of circulatory flow appearing in the layer and the magnitude of the characteristic quantity Ra beyond which the structure of the flow is reorganized. As the value of r_2/r_1 decreases, the characteristic Rayleigh number also decreases. Any nonuniformity in the flow field arises in the central part of the flow, moving at relatively low velocity.

From the data of [3] it follows that for a change from $r_2/r_1 = 1.4$ to $r_2/r_1 = 1.25$, which is the smallest ratio investigated in that study, the critical Grashof number for air decreases ($Gr_* \approx 5 \cdot 10^4$). In numerical calculations for min $r_2/r_1 = 1.1$ the transition value Gr_* remains practically in the same region, $10^5 \leqslant Gr \leqslant 2.5 \cdot 10^5$, as for $r_2/r_1 = 1.4$. Apparently this is due to the fact that the longitudinal temperature difference $(\Delta T)_\theta$, which has a substantial effect on the structure of the stationary motion, differs very little when $r_2/r_1 = 1.1$ from its value when $r_2/r_1 = 1.4$. The temperature distribution along the center line of the layer, $-\pi/2 \leqslant \theta \leqslant \pi/2$ with different value of r_2/r_1, is shown in Fig. 3, where the dashed curve corresponds to the temperature distribution in the heat-conduction regime for $r_2/r_1 = 2$. It can be seen that for a given value of the Grashof number the longitudinal temperature difference is determined by the ratio r_2/r_1. It has its maximum value when $r_2/r_1 = 1.4$ and decreases as r_2/r_1 increases. The longitudinal temperature gradient becomes stabilized. The secondary vortices ($r_2/r_1 = 1.4$) produce a wave-shaped variation in the temperature profile.

The influence of the radius ratio on the intensity of the flow is reflected in Fig. 4. The profiles for the angular velocity component v_θ are constructed as functions of the radius, $r_1 \leqslant r \leqslant r_2$, for one value of the angle $\theta = 0$. From the graph it follows that the absolute velocities of the ascending and descending flows for the smallest ratio r_2/r_1 are practically the same, and the hydrodynamic layers are not separated. These effects can be attributed to the relatively similar extent of the heated and cold surfaces. As r_2/r_1 increases, the absolute values of the velocities of the descending and ascending flows decrease. The maximum value of v for $r_2/r_1 = 1.1$ is almost three times its value for $r_2/r_1 = 5$. The shape of the profile also changes. On the cooled surface $r = r_1$ there is formed a narrow jet-shaped de-

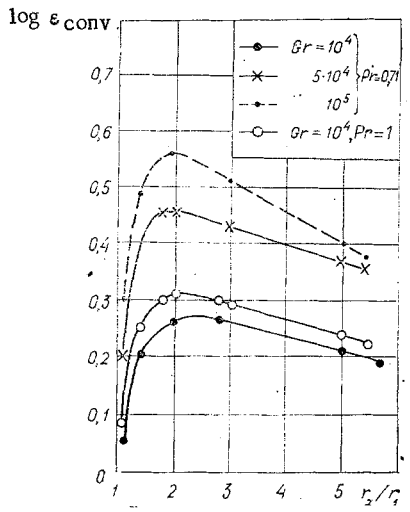

Fig. 5

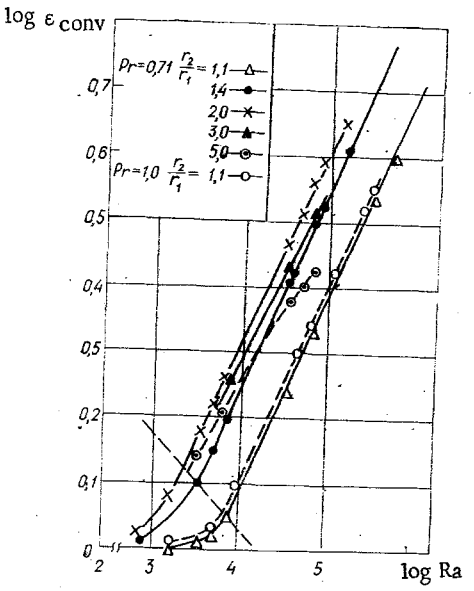

Fig. 6

scending flow, while the ascending flow becomes wider in accordance with the continuity equation. When $r_1/r_1 = 5$, the maximum velocity in the zone adjacent to $r = r_1$ is 3.5 times as high in absolute value as the extremum value of the velocity in the wide ascending flow. Thus, an increase in r_2/r_1 while Ra remains fixed leads to a decrease in the absolute values of the flow velocity, i.e., to a reduction in the intensity of motion.

The nature and the velocity of the liquid circulation in the wide and narrow layers also change the conditions of heat transfer through them. The influence of the relative thickness of the layer on the intensity of heat transfer has been investigated in detail for $Gr = 10^4$, $5\cdot10^4$, 10^5, $Pr = 0.7, 1.0$, and radius ratios of $r_2/r_1 = \delta/r_1 - 1 = 1.1, 1.4, 1.7, 2, 3, 5$. The results for the convection coefficient are shown in Fig. 5. It can be seen that the variation of ε_{conv} as a function of the ratio of radii is not monotonic. The variation of r_2/r_1 in the interval $1.1 \leqslant r_2/r_1 \leqslant 2$ leads to an intensification of the heat exchange. Here we observe a sharp increase in ε_{conv}, which becomes more pronounced as the Grashof number increases. In the vicinity of $r_2/r_1 = 2$ the function $\varepsilon_{conv}(r_2/r_1)$ takes on its maximum value. When $r_2/r_1 > 2$, the amount of heat removed by the flow gradually decreases. This type of variation of the convection coefficient is due to the choice of the range of variation of the ratio of radii and the behavior of ε_{conv} as r_2/r_1 tends to its limiting values.

As $r_2/r_1 \Rightarrow \infty$ $(r_1 \Rightarrow 0)$ the coefficient ε_{conv} will tend to its value in the case of heat transfer under conditions of a spherical cavity. However, if the temperature of the spherical surface is constant, then after the passage of some time interval (theoretically infinite) the liquid takes on the temperature of the surface and the heat transfer in the cavity will cease. In the other limiting case, when the values of r_2/r_1 are close to unity, we can expect that in the investigated range of Rayleigh numbers the heat transfer will take place only by conduction. These conclusions are confirmed by the data of Burelko and Shtessel' [9], who within the framework of similarity theory obtained a heat-transfer law for the case of free convection in cylindrical and spherical layers. The existence of a maximum of the function $\varepsilon_{conv} = \varepsilon_{conv}(r_2/r_1)$ is attributed by them to the competing influences of the Rayleigh number and the curvature of the region on the heat transfer.

The nonmonotonic nature of the variation of ε_{conv} as a function of the relative thickness of the layer, δ/r_1, must be taken into consideration when we select the optimal ratios of radii for minimizing the heat losses through the layers in structural elements.

The temperature stratification in the region leads to a nonuniformity in the distribution of the local heat fluxes along its boundaries, which increases with increasing r_2/r_1. Such a picture is qualitatively analogous to the distribution of heat fluxes when Gr increases in the case of $r_2/r_1 = \text{const}$ [5].

The results of the numerical solutions in the form of a function $\varepsilon_{conv}(Ra)$ for $Pr = 0.7$ and 1.0 and different ratios r_2/r_1 are shown in Fig. 6. The sequence in which the curves are arranged is the same in this case as in the case of natural convection of a gas in hori-

TABLE 1

Source	c	a	b	Range of parameters, Pr = 0.71
[2]	0,162	0,252	0,059	$2\cdot10^4 \leqslant Gr \leqslant 1{,}5\cdot10^7$ $1{,}25 \leqslant r_2/r_1 \leqslant 3{,}14$
Numerical method	0,158	0,266	0,057	$10^4 \leqslant Gr \leqslant 7\cdot10^5$ $1{,}1 \leqslant r_2/r_1 \leqslant 5$

zontal cylindrical layers [9]. For each r_2/r_1 we can determine from the graphs the value of the Rayleigh number corresponding to the transition from the conduction regime to a regime of fully developed convection. The values of Ra for this regime lie above the dashed curve. It can be seen from Fig. 6 that in narrow gaps (r_2/r_1 = 1.1 and 1.4) the regime of fully developed convection comes at higher values of the Rayleigh number than in wide gaps, i.e., a decrease in r_2/r_1 delays the development of the process. At the same time, the transition from one type of flow to the other, as noted above, takes place at lower Rayleigh numbers in the case of thin layers ($Ra \simeq 10^5$, r_2/r_1 = 1.4). From Figs. 5 and 6 it follows that for a given value of r_2/r_1 the convection coefficient increases with increasing Ra.

The nature of the curves in Fig. 6 enables us to generalize the data for a fully developed convection regime in the form of the following power function:

$$\varepsilon_{conv} = c\,\mathrm{Ra}^a\,(\delta/r_1)^b. \tag{8}$$

Using the method of least squares, we obtained the values of the constants appearing in this formula. They are shown in Table 1 together with the empirical constants from [2]. The exponent of r_2/r_1 practically coincides with the experimental value, but the dependence of the Rayleigh number is stronger than prediced by the experiment. The convection coefficients calculated from the experimental formula are 13.7% smaller (in modulus) on the average than those obtained by machine calculation. The reason for this, in addition to the difference in the range of parameters (see Table 1) may be that the experimental formula was obtained for the case of heating from within.

The mean deviation of the calculated values of the convection coefficient from those obtained by formula (8) is 11%. The maximum deviation does not exceed 24.5%, corresponding to r_2/r_1 = 5, and is apparently caused by the nonmonotonic variation of the convection coefficient as a function of r_2/r_1.

The mathematical processing of the data over the entire investigated range of parameters Pr and δ/r_1 in a regime of fully developed convection enabled us to obtain the criterion equation

$$\varepsilon_{conv} = 0.166\,\mathrm{Ra}^{0.262}\,\mathrm{Pr}^{0.04}(\delta/r_1)^{0.069}.$$

Since the exponent of the Prandtl number is small, we can assume with some error that the criteria Gr and Pr have equal influence on the intensity of the heat transfer. An analogous result was obtained in [6] for horizontal annular channels.

Thus, our numerical investigations enabled us to make clear the nonmonotonic nature of the variation of the convection coefficient as a function of the relative width of the gap and to find the form of the criterion equation of similarity in the range of parameters under consideration. We established that although the relative width of the gap does influence the intensity of the heat transfer, this influence is slight and may be disregarded in practical calculations.

LITERATURE CITED

1. E. H. Bishop, L. R. Mack, and J. A. Scanlan, "Heat transfer by natural convection between concentric spheres," Int. J. Heat Mass Transfer, 9, 649 (1966).
2. J. A. Scanlan, E. H. Bishop, and R. E. Powe, "Natural convection heat transfer between concentric spheres," Int. J. Heat Mass Transfer, 13, 1857 (1970).
3. S. H. Yin, R. E. Powe, et al. "Natural convection flow patterns in spherical annuli," Int. J. Heat Mass Transfer, 16, No. 9 (1973).
4. L. R. Mack and H. C. Hardee, "Natural convection between concentric spheres at low Rayleigh number," Int. J. Heat Mass Transfer, 11, 387 (1968).

5. G. B. Petrazhitskii and N. M. Stankevich, "Natural convection of a compressible fluid in spherical layers," Zh. Prikl. Mekh. Tekh. Fiz., No. 5 (1976).
6. G. B. Petrazhitskii, E. V. Bekneva, and N. M. Stankevich, "Calculation of flow and heat exchange in the free movement of a liquid in a horizontal annular channel," Voprosy Elektro- i Teploenergetiki, No. 46 (1970).
7. T. V. Kuskova, "A difference method for calculating flows in a viscous incompressible liquid," in: Computational Methods and Programming [in Russian], 7th edn., Moscow State University Press, Moscow (1967).
8. C. Y. Liu, W. K. Mueller, and F. Landis, "Natural convection heat transfer in horizontal cylindrical annuli," Int. Developments in Heat Transfer, pt. 5, No. 117 (1961).
9. V. V. Burelko and É. A. Shtessel', "Heat transmission by natural convection in cylindrical and spherical interlayers," Inzh.-Fiz. Zh., 24, No. 1 (1973).